

# Composition and microstructure of alkali activated fly ash binder: Effect of the activator

A. Fernández-Jiménez\*, A. Palomo

*Eduardo Torroja Institute (CSIC), 28080 Madrid, Spain*

Received 21 February 2005; accepted 29 March 2005

## Abstract

The alkali activation of fly ashes is a chemical process by which the glassy component of these powdered materials is transformed into very well-compacted cement. In the present work the relationship between the mineralogical and microstructural characteristics of alkaline activated fly ash mortars (activated with NaOH, Na<sub>2</sub>CO<sub>3</sub> and waterglass solutions) and its mechanical properties has been established. The results of the investigation show that in all cases (whatever the activator used) the main reaction product formed is an alkaline aluminosilicate gel, with low-ordered crystalline structure. This product is responsible for the excellent mechanical-cementitious properties of the activated fly ash. However the microstructure as well as the Si/Al and Na/Al ratios of the aluminosilicate gel change as a function of the activator type used in the system. As a secondary reaction product some zeolites are formed. The nature and composition of these zeolites also depend on the type of activator used.

© 2005 Elsevier Ltd. All rights reserved.

**Keywords:** Alkali activation; Fly ash; Microstructure

## 1. Introduction

Power stations, using coal like-fuel are worldwide energy sources; so, significant quantities of fly ashes are generated (it is considered that the volume of fly ashes production will reach the 800 Mtons in 2010). Only a small part of these ashes is used at present (20–30%); the rest is stored giving serious space problems, potential risks of air pollution, contamination of water due to leaching, etc.

Nevertheless important advances in the search for new applications for the fly ashes are being achieved. Among the main achievements, a new type of binder named “alkaline cement” should be mentioned [1–11].

The process of activation of fly ashes allows to obtain of a material with similar cementing features than those characterising ordinary portland cement. But this process is also the origin of important economical and environ-

mental benefits when compared with the traditional manufacture of OPC, the emissions of CO<sub>2</sub> to the atmosphere would decrease, the energy consumption would also decrease, the destruction of natural quarries would be attenuated, etc.).

The alkali activation of fly ashes (AAFA) is a particular procedure by which the grey powder (FA) is mixed with certain alkaline activators (alkaline solutions) and then the mixture is cured under a certain temperature to make solid materials. The glassy constituent of the fly ash is transformed into a well-compacted cement. In previous works [4,8,13], it was found that the main reaction product formed in AAFA is an amorphous aluminosilicate gel. This product, also considered as a “zeolite precursor”, is a X-ray amorphous material difficult to characterise. According to our investigations [13], the zeolites crystallisation might be at long term, the hypothetical final stage of the alkali activated fly ashes.

The “zeolite precursor” has a short-range order for which a 3-dimensional structure where the Si occurs in a variety of environments with a predominance of Q<sup>4</sup> (3Al)

\* Corresponding author.

E-mail address: [pesfj18@ietcc.csic.es](mailto:pesfj18@ietcc.csic.es) (A. Fernández-Jiménez).

and  $Q^4$  (2Al), has been deduced [8,13]. Additionally the presence of a small content of some zeolites type hydroxysodalite, herchelite, etc. has also been detected in this type of systems [4].

Palomo et al. [4,8] also found that different fly ashes activated with NaOH 8–12 M cured at 85 °C for 24 h produced a material with compressive mechanical strengths between 35–40 MPa and about 90 MPa if some waterglass was added to the NaOH solution ( $SiO_2/Na_2O=1.23$ ) [4,8]. Xie and Yunping [7] indicated that the hardening process of the fly ashes activated with a waterglass solution ( $SiO_2/Na_2O=1.64$ ), should mainly be attributed to the gel-like reaction products that bind the particles of fly ash together.

Additionally, in the bibliography many references about zeolite synthesis by alkali hydrothermal reaction of coal fly ashes can be found [14–17]. In these works it has been already explained that the type of zeolite formed at the end of the process will mainly depend on the experimental conditions (nature and concentration of the activator, curing temperature and curing pressure, “solid/liquid” ratio, etc.). For example, LaRosa et al. [15] found that zeolite Na–P and zeolite Y were formed when they used NaOH solution as activator, but no zeolites were formed when a KOH solution was applied in their systems. However Murayama et al. [16] found zeolite P and chabazite from coal fly ash when using NaOH,  $Na_2CO_3$  and KOH solutions.

In conclusion, the activation process of fly ashes when oriented towards the production of a cementitious material could be considered like a “zeolitisation” process in which the last stage (crystallisation stage) is not reached, due to our experimental conditions, which force very fast reaction rates at the beginning of the process (dissolution and condensation step) but an extremely slow reaction rate after the hardening of the material occurs [13].

The present paper is focused towards advancing the knowledge about this process of alkali activation of fly ashes when the production of a cementitious material is aimed for. The specific objective was the study of the effect of the type of activator on the mechanical strength of alkali activated fly ash mortars and on the nature and microstructure of the reaction products.

## 2. Experimental

A Spanish fly ash (type F according to the ASTM classification) derived from anthracite and soft coal has been

Table 2  
Samples composition

Activator	Sample	Sol./FA (in mass) <sup>a</sup>	[Na <sub>2</sub> O], % <sup>b</sup>	[SiO <sub>2</sub> ], % <sup>b</sup>	[CO <sub>3</sub> <sup>2-</sup> ], % <sup>b</sup>	SiO <sub>2</sub> / Na <sub>2</sub> O <sup>b</sup>
NaOH	FAN12	0.35	13.67	–	–	–
	FAN8	0.35	8.68	–	–	–
	FAN6	0.35	6.51	–	–	–
NaOH+ waterglass	FAW8	0.35	7.74	9.52	–	1.23
	FAW75	0.35	5.55	7.14	–	1.28
	FAW20	0.4	13.00	2.22	–	0.17
	FAW15	0.4	14.09	1.67	–	0.118
	FAW10	0.4	14.28	1.11	–	0.078
	FAW5	0.4	14.90	0.56	–	0.037
NaOH+ $Na_2CO_3$	FAC8	0.35	8.68	–	6	–

<sup>a</sup> “Solution/fly ash” ratio (in mass).

<sup>b</sup> Percentage with respect to fly ash content (in mass).

used in this investigation. The chemical analysis is given in Table 1, but complete characterisation of this fly ash can be found in Ref. [12]. In any case it is important to remark that this fly ash contains, approximately, 90% of particles sized lower than 45 µm and 50% lower than 10 µm.

For the preparation of the alkaline solutions three different alkaline compounds were used: NaOH (98% purity), sodium silicate (8.2%  $Na_2O$ , 27%  $SiO_2$  and 64.8%  $H_2O$ ,  $d=1.38$  g/cm<sup>3</sup>) and anhydrous sodium carbonate (98% purity); all of them supplied by PANREAC S.A. The detailed concentration of each solution is given in Table 2.

The mortars resulting from mixing the fly ash with the sand and the alkaline solution were poured into metallic prismatic moulds (4×4×16 cm), which were later kept in an oven at 85 °C for 20 h. After that, demoulding of the specimens was carried out and finally the prisms were submitted to flexural and compressive failure according to the Spanish standard UNE-80-101-88 (an aggregate/fly ash ratio of 2:1 was used).

The mineralogical and microstructural characteristics of the materials were studied by means of XRD, FTIR, and SEM/EDX. X-ray diffractograms of powdered samples were obtained with a Philips diffractometer PW 1730, using  $CuK\alpha$  radiation. Specimens were step-scanned at a rate of 2°/min, with  $2\theta$  in the range 2–60°, divergence slit=1°, anti-scatter slit=1° and receiving slit=0.1 mm. FTIR spectra were obtained on an ATIMATTSON FTIR-TM series spectrophotometer. Specimens were prepared by mixing 1 mg of sample in 300 mg of KBr. Spectral analysis was performed over the range 4000–400 cm<sup>−1</sup> at a resolution of 1 cm<sup>−1</sup>. Finally a JEOL JSM 5400 scanning

Table 1  
Chemical composition of fly ash

	L.o.I. <sup>a</sup>	IR <sup>b</sup>	SiO <sub>2</sub>	Al <sub>2</sub> O <sub>3</sub>	Fe <sub>2</sub> O <sub>3</sub>	CaO	MgO	SO <sub>3</sub>	K <sub>2</sub> O	Na <sub>2</sub> O	TiO <sub>2</sub>	SiO <sub>2</sub> reactive <sup>c</sup>
Fly ash	3.59	0.32	53.09	24.80	8.01	2.44	1.94	0.23	3.78	0.73	1.07	50.44

<sup>a</sup> L.o.I.=Loss on ignition.

<sup>b</sup> IR=Insoluble Residue.

<sup>c</sup> Reactive  $SiO_2$  calculated according to the Spanish standard UNE 80-225-93.

electron microscope equipped with a LINK-ISIS energy dispersive (EDX) analyser was used for microstructural characterisation.

### 3. Results

#### 3.1. Mechanical strength of AAFA cement mortars

In Table 3 flexural and compressive mechanical strengths of alkaline activated fly ash (AAFA) mortar prisms are given.

For preparing the mortar prisms some different strongly alkaline solutions ( $\text{pH} > 12$ ) were employed. The content of  $\text{Na}_2\text{O}$  in those solutions ranged between 5% and 15% in mass with respect to the content of fly ash (see Table 2). Data from Table 3 indicate that the  $\text{Na}_2\text{O}$  content plays an important role in the development of mechanical strength of the system. When the activator is a NaOH solution (see samples FAN12, FAN8 and FAN6), increasing the concentration of  $\text{Na}_2\text{O}$  corresponds to an increase in mechanical strength. For the particular case of sample FAN12, a compressive strength of 70.4 MPa was achieved.

But also, the presence in the system of soluble silica notably affects the development of mechanical strength of the material. In fact, sometimes even more than 90 MPa in compression, after 20-h curing, can be achieved. Moreover in such cases not only the  $\text{SiO}_2/\text{Na}_2\text{O}$  ratio is a very important parameter, but the “water to binder ratio” is also an important variable to take into account. When the “Sol./FA” ratio is 0.35, the increase of the ratio “ $\text{SiO}_2/\text{Na}_2\text{O}$ ” from 1.23 to 1.28 involves the decrease of the mechanical strength from 82.36 to 56.23 MPa. It is because of the low content of  $\text{Na}_2\text{O}$  in the sample FAW75 (5.55%) that makes the pH of the solution to decrease and consequently negatively affecting to the kinetics of the reaction [4] and therefore the development of mechanical strengths. Nevertheless, the highest mechanical strengths correspond to the sample FAW15 with a “Sol./FA”=0.4 and a ratio “ $\text{SiO}_2/\text{Na}_2\text{O}$ ”=0.118. If “ $\text{SiO}_2/\text{Na}_2\text{O}$ ” is lower or higher than 0.118, mechanical strengths fall down. These results are in good agreement with those published by Xie et al. [7]. In any case in Table 3, it can be observed that the highest

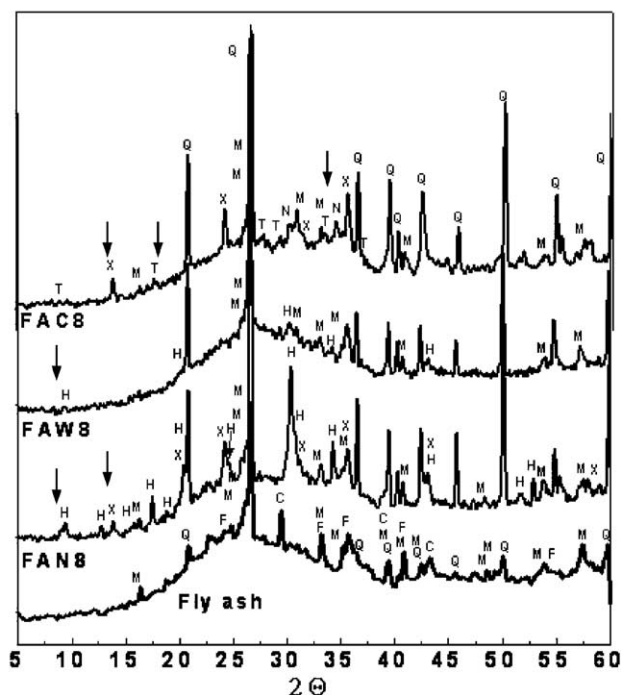


Fig. 1. XRD of alkali activated fly ash mortars; Q=quartz from fly ash and aggregate; M=Mullite; F=hematite; C=CaO; H=herchelite; X=hydroxysodalite; T=trona; N=nahcolite.

mechanical strengths correspond to samples FAW8 and FAW15 with ratios “ $\text{SiO}_2/\text{Na}_2\text{O}$ ” respectively 1.23 and 0.12. That is the reason why we consider that total amounts of  $\text{Na}_2\text{O}$  and  $\text{SiO}_2$  are also critical parameters.

Finally, the presence of  $[\text{CO}_3^{2-}]$  in the activating solution corresponds to materials with relatively low mechanical strengths (around 35 MPa), even if high contents of  $\text{Na}_2\text{O}$  are available in the samples.

#### 3.2. Mineralogical and microstructural characterisation

The reasons explaining the different mechanical behaviors of mortar prisms as a function of the activator used are closely related to the mineralogy and microstructure of the cementing component of the materials. It is for this reason that we planned a detailed study of samples FAN8, FAW8 and FAC8, all of them presenting a similar content of  $\text{Na}_2\text{O}$ .

Results obtained by XRD (see Fig. 1) show that the original fly ash is basically constituted of a major vitreous phase (hump registered between  $2\theta = 20^\circ$  and  $2\theta = 30^\circ$ ) and of some minor crystalline phases (quartz, mullite, hematite, magnetite and some CaO).

In Fig. 1, the XRD patterns of FAN8, FAW8 and FAC8 are also shown. When the fly ash is activated according to the previously mentioned conditions, whatever the activating solution used, the main reaction product formed is that already mentioned “alkaline aluminosilicate gel” with low-order crystalline structure [4,13], which does not pattern but appears with low and scattered bands. This hump, in the XRD diffractogrammes overlaps partially with that of the

Table 3  
Mechanical strengths

Sample	Strength (MPa)		Sample	Strength (MPa)	
	Flexural	Comp.		Flexural	Comp.
FAN12	12.3	70.4	FAW8 <sup>a</sup>	8.9	82.36
FAN8 <sup>a</sup>	4.6	42.07	FAW75	7.94	56.23
FAN6	4.4	32.0	FAW20	7.8	65.7
			FAW15	8.2	91.6
FAC8 <sup>a</sup>	5.08	35.99	FAW10	7.9	73.6
	FAW5	6.6			54.5

<sup>a</sup> Samples submitted to further mineralogical and microstructural study.

original ash, however it appears slightly shifted toward higher values (between  $2\theta = 25\text{--}35^\circ$ ).

Comparing the XRD spectra of the original fly ash with those of the hardened materials, it can be seen that the crystalline phases originally existing in the fly ash (quartz, mullite, etc.) have not been apparently altered by the activation reactions. Maybe those diffraction lines associated with the presence of quartz appear more intensely in the samples corresponding to the activated fly ash than in the original fly ash but this is probably due to some particle of sand, which could not be totally eliminated from the mortars when samples were prepared for XRD analysis. In any case, some authors [19] believe that mullite and quartz are slightly altered when submitted to such strong alkaline medium. However, one of the most important data collected in this investigation were observed in the XRD patterns: Some minor crystalline phases (zeolites) exist in the activated ash samples.

The XRD pattern of sample FAN8 (8.68% of  $\text{Na}_2\text{O}$ , 0% of  $\text{SiO}_2$ ) presents some intense peaks associated with the presence of zeolites like hydroxysodalite ( $\text{Na}_4\text{Al}_3\text{Si}_3\text{O}_{12}\text{OH}$ ) and especially herschelite ( $\text{NaAlSi}_2\text{O}_6 \cdot 3\text{H}_2\text{O}$ ). In sample FAW8 (7.74% of  $\text{Na}_2\text{O}$  and 9.52% of  $\text{SiO}_2$ ), through XRD only the formation of herschelite is detected (and the peaks are not so intense as in sample FAN8). Finally the XRD pattern of sample FAC8 (8.68% of  $\text{Na}_2\text{O}$  and 6%  $\text{CO}_3^{2-}$ ) shows the presence of hydroxysodalite as the only zeolite crystallised. In this case, the presence of little amounts of sodium bicarbonate like Trona ( $\text{Na}_2\text{H}[\text{CO}_3]_2 \cdot 2\text{H}_2\text{O}$ ) and Nahcolite ( $\text{NaHCO}_3$ ) was also detected (see Fig. 1).

The FTIR spectrum of the original fly ash as well as those spectra belonging to the alkali activated fly ashes are shown in Fig. 2. The fly ash FTIR spectrum shows one broad component at  $1060\text{ cm}^{-1}$ , ascribed to T–O stretching vibrations (T=Si or Al) and another located at  $454\text{ cm}^{-1}$  ascribed to  $\nu_4(\text{O}(\text{Si}(\text{O}))$  bending modes of  $\text{SiO}_4$  tetrahedra [4,20].

In the FTIR spectra of samples corresponding to the alkali activated fly ash, the main adsorption bands were as follows: 1172, 1084, 798, 780,  $697\text{ cm}^{-1}$  (see peaks Nos. 1, 2, 3, 4 and 5 in Fig. 2). They are produced by the quartz forming part of fly ash, but also by the aggregate (“sand-quartz”) forming part of the mortar and not completely eliminated from samples.

On the other hand the activation reaction of the fly ash hardly affects the band at  $454\text{ cm}^{-1}$   $\nu_4(\text{O}(\text{Si}(\text{O}))$ , since it almost does not change the position. This band (No. 7, at Fig. 2) provides an indication of the degree of “amorphisation” of the material, since its intensity does not depend on the degree of crystallisation [20]. However the band T–O at  $1060\text{ cm}^{-1}$  of the original fly ash becomes sharper and shifts towards lower frequencies in the whole activated materials: 1019 (FAN8), 1024 (FAW8) and  $1005\text{ cm}^{-1}$  (FAC8) (see Fig. 2, No. 6). All these displacements are indicating that the vitreous component of the fly ash is reacting with the alkali activator and therefore that new

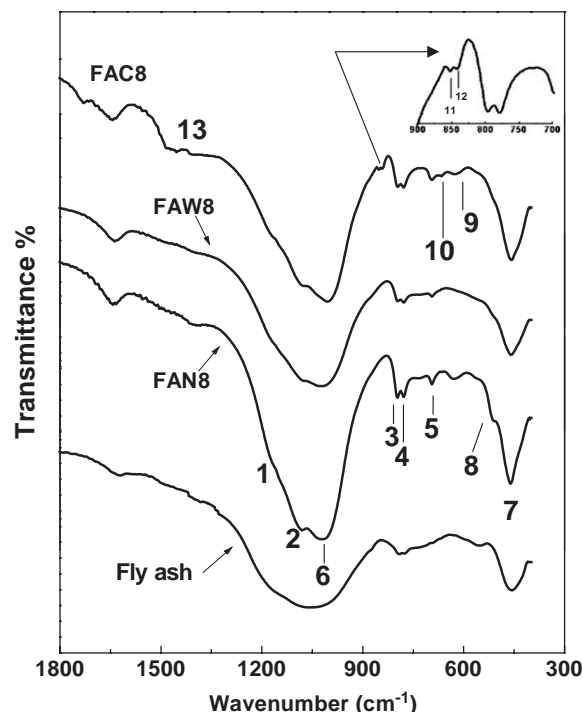


Fig. 2. FTIR spectra of fly ash and alkali activated fly ash mortars.

products of reaction are being formed (the main one: the alkaline aluminosilicate gel). Comparing the shift of the band T–O for the different samples it has been observed that matrix FAW8 ( $1024\text{ cm}^{-1}$ ) is the one at which the displacement has taken place more intensely. This is indicating that the reaction product of FAW8 has a Si contents higher than the reaction products of FAN8 and FAC8 (this way of interpretation of IR bands displacements is in good agreement with Refs. [20,21]).

Those bands appearing at 509, 629 y  $665\text{ cm}^{-1}$  in the spectrum FAN8 (see Fig. 2, Nos. 8, 9, 10) and those bands appearing at 625 and  $665\text{ cm}^{-1}$  in the spectrum FAC8 have all been associated with the presence of zeolites [20,21] (already detected through XRD). Finally in the spectrum FAC8, the existence of a double band at 851 and  $841\text{ cm}^{-1}$  (see Fig. 2, Nos. 11, 12) together with a band towards  $1453\text{ cm}^{-1}$  (No 13) has been assigned to the presence of sodium bicarbonates (Trona: band in  $851\text{ cm}^{-1}$ ; and Nahcolite: band in  $841\text{ cm}^{-1}$ ).

Of course, in all cases, stretching and deformation modes of water were detected at 3500 and  $1600\text{ cm}^{-1}$ .

Finally, Figs. 3, 4 and 5 correspond to a set of SEM pictures not only showing interesting morphological aspects of the studied systems but also contributing to clarify the mechanisms through which reactions take place as a function of the activator used. The figures also give information on the chemical composition of the products of reaction (see Table 4) and on the degree of reaction achieved by the systems. In this sense we must mention that in previous investigations it was already concluded that by applying similar experimental conditions to the ones applied



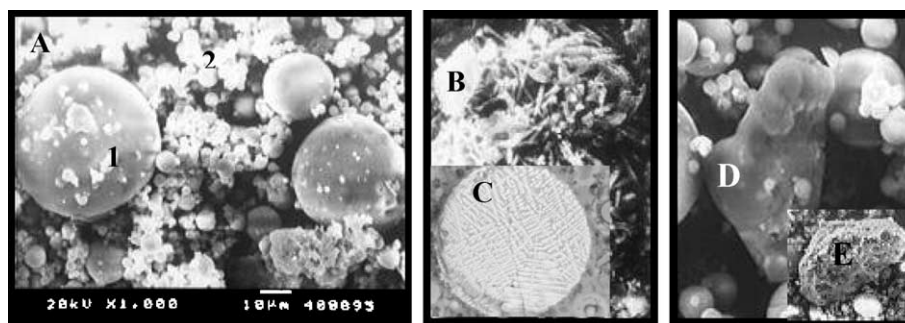


Fig. 3. Un-reacted fly ash.

in this work, the usual evolution of this type of systems is to achieve degrees of reaction around 50% [13,18,20].

Micrographs in Fig. 3 are showing the general features of the original fly ash before the activation takes place. As it can be seen in the figure, the fly ash is mainly constituted by compact or hollowed spheres of different size (Fig. 3A, points 1 and 2) but with a regular smooth texture. Often, on the spheres surface the existence of solid deposits or small crystals can be observed: soluble alkaline sulphates, dendritic-shaped particles of iron minerals (Fig. 3C), mullite crystals (Fig. 3B), etc. Also some quartz particles (Fig. 3D), some residue of unburned coal (Fig. 3E), or some vitreous unshaped fragments, can be seen.

In Fig. 4 the microstructure of mortar FAN8 (fly ash activated with 8.68% of  $\text{Na}_2\text{O}$ ) is presented: Together with the unreacted spheres (point 3), there exists the amorphous aluminosilicate gel (points 4 and 5). From the EDX analysis (see Table 4), an averaged compositional ratios of “Si/

Al”=1.6–1.8 and “Na/Al”=0.46–0.68 has been deduced for that gel.

The considerable amount of unreacted or not totally consumed spheres is indicating a moderate degree of reaction in the system. In point 6 of Fig. 4B, over the main matrix of reaction product, some deposits (apparently crystalline material) can be observed. These deposits probably correspond to a more advanced or developed stage of the aluminosilicate gel: They contain more Si and less Al than the main matrix (Si/Al=1.9 and Na/Al=1.22, as deduced from Table 4), which is in accordance with previous works [8,13]. Also in Fig. 4A, some tracks belonging to spheres previously occupying that space can be seen.

From Fig. 4, and according with previous experience [13,20,22], we have estimated that the activation level of the fly ash (reaction degree) with the NaOH solution, in the particular experimental conditions of this investigation, has

Table 4  
EDX microanalysis on specific points of the samples (atomic data)<sup>a</sup>

Sample	Point	Na	Al	Si	K	Ca	Fe	Si/Al	Na/Al
Fly ash	1	1.65	11.27	20.46	1.53	0.64	1.76	1.81	0.15
	2	0.26	10.16	20.46	1.80	0.64	2.41	2.01	0.025
FAN8 (8.68% $\text{Na}_2\text{O}$ )	3	2.95	11.63	20.43	1.96	0.11	0.81	1.76	0.25
	4	4.85	10.50	19.71	2.31	0.22	1.38	1.88	0.46
	5	7.55	11.10	18.01	1.60	0.28	1.29	1.62	0.68
	6	11.16	9.16	17.54	1.57	0.67	0.99	1.91	1.22
	7	10.99	8.38	18.11	1.87	0.79	1.16	2.16	1.31
	8	10.54	8.17	17.73	1.44	1.71	1.33	2.17	1.29
FAW8 (7.74% $\text{Na}_2\text{O}$ 9.52% $\text{SiO}_2$ )	9	10.58	7.07	17.98	1.03	2.06	0.95	2.54	1.50
	10	11.72	4.17	19.51	1.33	0.55	0.64	2.72	1.63
	11	10.99	7.01	19.92	1.27	0.52	0.70	2.84	1.57
	12	5.85	6.48	21.75	1.98	0.77	1.34	3.35	0.90
	13	9.54	8.44	18.89	1.30	0.45	0.97	2.24	1.13
	14	7.21	8.54	19.94	1.89	0.63	1.14	2.33	0.84
FAC8 (8.68 $\text{Na}_2\text{O}$ and 6% $\text{CO}_3^{2-}$ )	15	11.21	9.02	18.13	1.54	0.57	1.12	2.01	1.24
	16	9.71	8.76	18.77	1.63	0.46	1.10	2.15	1.11
	17	13.09	8.50	17.44	1.42	0.23	1.17	2.05	1.54
	18	13.03	8.12	17.67	1.50	0.36	0.95	2.18	1.60
	19	13.49	8.75	16.61	0.98	1.03	1.07	1.90	1.54
	20	13.18	6.37	16.17	1.35	1.28	2.90	2.54	2.07
	21	23.7	6.84	13.16	0.79	0.31	0.48	1.92	3.46
	22	26.51	4.29	10.95	0.80	2.76	1.04	2.55	6.18
	23	16.43	7.72	16.38	1.67	0.24	1.28	2.12	2.13
	24	31.99	3.98	11.16	0.68	0.25	0.34	2.80	8.04

<sup>a</sup> The variability in EDS analysis is  $\pm 1$ .

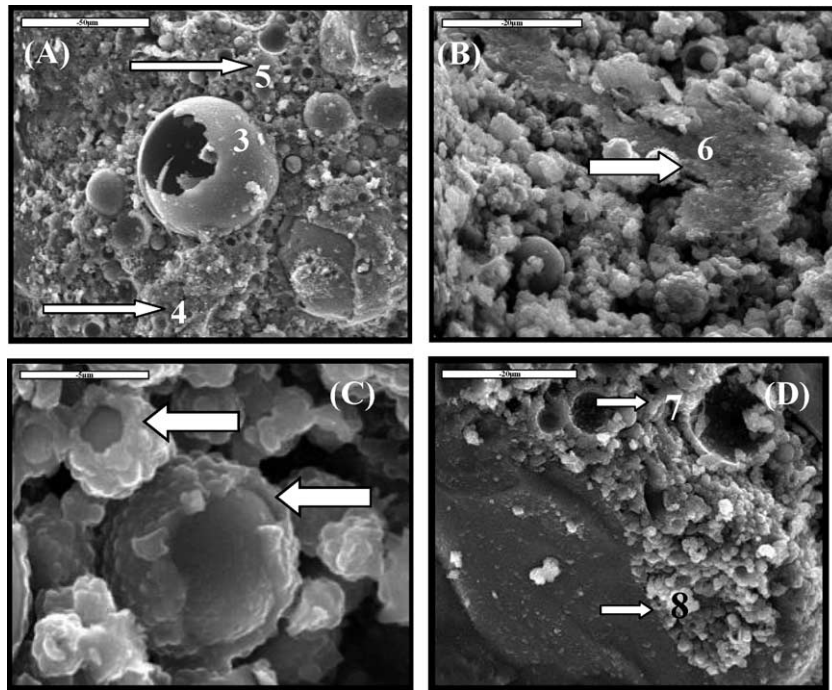


Fig. 4. Sample FAN8. SEM micrographs of alkali activated fly ash mortars with 8.68% of  $\text{Na}_2\text{O}$ .

become only moderate: the cementitious matrix presents significant number of pores. In Fig. 4C some ash spheres partially covered with reaction product are arrowed. This picture might be suggesting that the precipitation of the reaction products forms, in a short period of time, a layer on still unreacted spheres, which would inhibit its activation. This fact could justify the moderate degree of reaction already observed in this type of systems [13].

Finally through Fig. 4D, a little group of bright particles (probably zeolite crystals) was detected (see points 7 and 8). These particles are richer in Na and Si than the bulk of the amorphous matrix ( $\text{Si}/\text{Al}=2.16$  and  $\text{Na}/\text{Al}=1.3$  as deduced from Table 4). In this particular picture it is also observed that the interfacial area between the aggregate and the aluminosilicate gel matrix is almost non-existent which could mean that the adherence of the cementitious material with the aggregates is really good.

By means of the pictures at Fig. 5 the microstructure of mortar FAW8 (fly ash activated with 7.74% of  $\text{Na}_2\text{O}$  and

9.52%  $\text{SiO}_2$ ) can be described. It is rapidly observed that the morphology of the cementing matrix at FAW8 is clearly different from the previously described at FAN8. Now, in Fig. 5 a very compact material with almost no pores is observed. The superficial continuity of the mass of reaction product appears like a layer of a viscous fluid suddenly frozen (instead of a group of individual particles randomly precipitated which could describe a traditional cementitious system). Occasionally some cracking is observed (see point 11 in Fig. 5). These cracks might be due to mechanical damage during sample preparation for SEM observation or, mainly, to the thermal treatment carried out during the activation process. EDX analysis confirms this matrix has higher  $\text{Si}/\text{Al}$  and  $\text{Na}/\text{Al}$  ratios (about 2.7 and 1.5, respectively, see Table 4) than the product formed when the activator is a  $\text{NaOH}$  solution.

Also we must indicate that no zeolite crystals were detected through the SEM observations of sample FAW8 in spite of herschelite being detected by XRD. It could be due

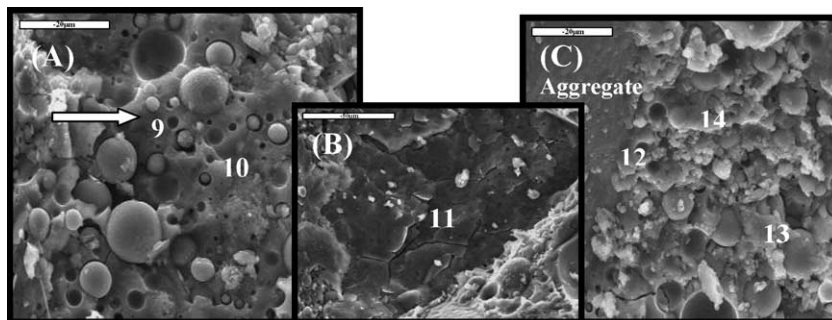


Fig. 5. Sample FAW8. SEM micrographs of alkali activated fly ash mortars with 7.74% of  $\text{Na}_2\text{O}$  and 9.52%  $\text{SiO}_2$ .

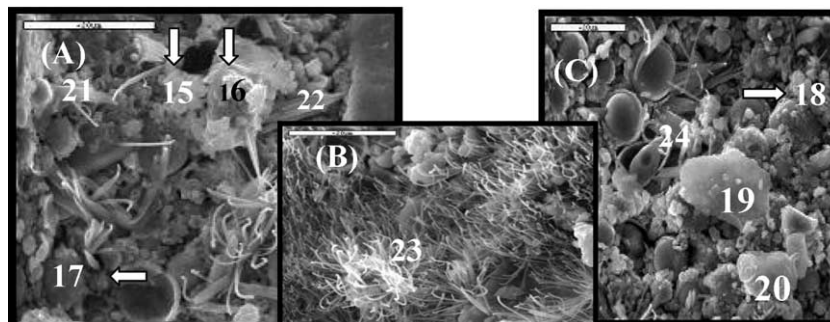


Fig. 6. Sample FAC8. SEM micrographs of alkali activated fly ash mortars with 8.68% of  $\text{Na}_2\text{O}$  and 6% of  $\text{CO}_3^{2-}$ .

to a very small size of the zeolite crystals. In Fig. 5C, again, a very good adherence between aggregate and matrix is observed.

Finally, in Fig. 6 the morphological characteristics of mortar FAC8 (ash activated with 8.68%  $\text{Na}_2\text{O}$  and sodium carbonate) are presented. This material is the most porous one among those studied. The main reaction product, in this case, presents a Si/Al ratio of 2.0–2.1 and a Na/Al ratio of 1.0 (see Fig. 6, points 16, 17, 18, 3); that is to say: this material possesses a chemical composition which can be considered as intermediate between the FAW8 and FAN8. Points 19 and 20 are associated to the presence of zeolitic crystals (particles having defined edges and different sizes and Si/Al=2.54 and Al/Na=2.07).

In this case the appearance of a group of needle shaped grey-white, transparent to translucent, crystals must be emphasised (Points 21, 22, 23 and 24). They have a high amount of sodium (15–30%). These uniform unmistakable crystals occupying large space are associated with the presence of Trona and Nahcolite detected by XRD, and FTIR.

#### 4. Discussion

The study of the alkali activation process of fly ashes as a method of synthesis of new cementitious materials is gaining relevance in the scientific community. The increasing number of scientific publications as well as the number of international events monographically dedicated to this particular subject are a proof of it. On the other hand the alkali activation of fly ashes is a process narrowly related to the synthesis of zeolites. In this sense Nurayama et al. [16] established in 2002, a global model for describing the synthesis of zeolites by which the dissolution of  $\text{Si}^{4+}$  and  $\text{Al}^{3+}$  from coal fly ash takes place firstly followed by a condensation step of silicate and aluminate ions where the aluminosilicate gel precipitates. Finally, according to this author the crystallisation of zeolites occurs.

As it has been indicated in previous works [13,20,22], the AAFA process evolves through different stages. On the other hand the first stage can also be divided into two sub-stages respectively named: Destruction–Coagulation and

Coagulation–Condensation. The main differences between traditional zeolitic systems and alkaline activated binding systems come from the distinct experimental conditions employed in the each synthesis process. In the case of the activation of the fly ashes low “liquid/solid” ratios and very high  $\text{OH}^-$  concentrations are employed. These particular conditions lead to a situation in which the crystal growth from the zeolitic nuclei formed (second stage) is extremely slow and therefore, an amorphous cementitious matrix (alumino-silicate gel or “zeolite precursor”) is initially stabilized. In any case small amounts of zeolite crystals are detected to form part of our cementitious material. Its presence is probably indicating that crystalline zeolites are the thermodynamically stable phases towards which the system should evolve with time.

The mechanism controlling the chemical reaction giving place to the prezeolite gel is initially associated to a dissolution process (the high concentration of  $\text{OH}^-$  ions in the system is responsible of the breakdown of the Si–O–Si, Si–O–Al and Al–O–Al bonds forming part of the vitreous phase of the ash and therefore of the formation of Si–OH and Al–OH groups). Later on these chemical species condense giving place to the precipitation of zeolitic precursor. This gel possesses a 3-dimensional structure with a zeolitic order at short range [1,4,13].

During this chemical process, the role played by the alkaline metals being incorporated to the system should be remarked. This role is essential since monovalent metals compensate the electrical load of the microstructure when  $\text{Al}^{3+}$  atoms replace  $\text{Si}^{4+}$ .

In summary, the main reaction product formed in all the cases faced in this investigation is that alkaline aluminosilicate gel (or “prezeolite”). However, the presence, in the alkaline system, of different types of anions, can induce relevant differences in the final chemical composition of that gel.

When the activating solution includes  $\text{Na}^+$  and also soluble  $\text{Si}^{4+}$  (sample FAW8), both elements are incorporated in the reaction products. The final result is a matrix having Si/Al=2.7 and Na/Al=1.5. These ratios are clearly higher than those found with the other two activators (see Fig. 7). In summary, the addition of waterglass to the activating solution enhances the polymerisation process of the ionic



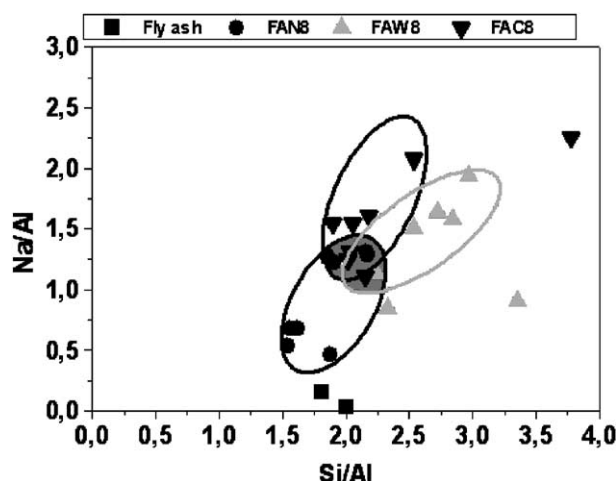


Fig. 7. SEM/EDX analysis of the original fly ash and activated samples.

species present in the system, which has been confirmed by the FTIR data (the band T–O appearing at  $1024\text{ cm}^{-1}$  is slightly shifted towards lower frequencies with respect the original fly ash). It simultaneously justifies the existence of some FAW samples developing very high mechanical strengths. Nevertheless, it should be emphasised that an activating solution made of NaOH+waterglass must be optimised in terms of defining not only the  $\text{SiO}_2/\text{Na}_2\text{O}$  ratio but also the total amount of  $\text{Na}_2\text{O}$  and  $\text{SiO}_2$  in the solution, because a threshold value exists ( $\text{Na}_2\text{O} > 7\%$  and  $\text{SiO}_2 > 1\%$ ) above or below which mechanical strength development at 20 h is below 65 MPa (see Tables 2 and 3). In other words, equilibrium between NaOH and waterglass in the solution should be reached in order to maintain the system with a high pH and a high level of soluble  $\text{Si}^{4+}$ .

When the activating solution is a mixture of NaOH+ $\text{Na}_2\text{CO}_3$ , the main modification induced to the system is the incorporation of carbonate to the mixture, which promotes the formation of sodium bicarbonate (Trona and/or Nahcolite) among the reaction products (see Fig. 1). It involves an acidification of the medium leading, consequently, to a relatively low amount of Al and Si dissolved from the fly ash. This could explain why FAC samples show a very porous microstructure and low mechanical strengths for similar reaction periods than FAW and FAN materials. However, it can be deduced from Fig. 7 that the main product of reaction in this case (the amorphous aluminosilicate gel) presents a “Si/Al” ratio around 2–2.1 and a “Na/Al” ratio around 1. These ratios are somewhat lower than in the case of the previously discussed activator (NaOH+Waterglass), which means a lower degree of polymerisation of the zeolitic precursor (as expected, since now we are not directly incorporating soluble  $\text{Si}^{4+}$  in the system). But additionally, these ratios are somewhat higher than in the case of the matrix produced with an activator made only of NaOH. What we interpret is that the presence of carbonate ions in the reactive system has the effect of acting as a promoter of the condensation of the species and consequently of stimulating the polymerisation of the aluminosilicate gel.

This result is in good agreement with those investigations attributing to a certain number of “promoters” ions ( $\text{PO}_4^{3-}$ ,  $\text{NO}_3^-$ ,  $\text{CO}_3^{2-}$ ,  $\text{SO}_4^{2-}$ , etc.) capacities to accelerate the crystallisation rate of certain zeolite structures [23,24]. Naturally, the production of a highly polymerised material should lead to cement with high mechanical strength. But in this case, the rate of the reactions drops too soon due to the high decrease of the pH of the system.

When a NaOH solution is used as the activating element of the fly ash, the main product of reaction presents low Si/Al ratio (1.8–1.8) and low Na/Al ratio (0.46–0.68) (see Fig. 7). In spite of this, mechanical strengths of FAN matrices are reasonably good. It is because this particular system maintains a very high  $\text{OH}^-$  concentration during the activation process.

Finally, it is quite interesting to observe in Fig. 7 the compositional common area (greyish plotted) for the matrices made with the different activators. That overlapped area coincides with the composition of herschelite (a type of zeolite also name chabazite-Na). This zeolite is present in most of our materials and has already been detected in previous works related with the study of AAFA systems [13,20,22].

## 5. Conclusions

The main reaction product of alkali-activated fly ash is an alkaline silicoaluminate gel.  $\text{OH}^-$  ion acts as a reaction catalyst during the activation process; and the alkaline metal ( $\text{Na}^+$ ) acts as a structure-forming element. The structure of the prezeolite gel contains Si and Al tetrahedral randomly distributed along the polymeric chains that are cross-linked so as to provide cavities of sufficient size to accommodate the charge balancing hydrated sodium ions. When the alkali activator is a NaOH solution, the “sodium aluminosilicate gel” presents a Si/Al=1.6–1.8 and Na/Al=0.46–0.68 ratio. In the presence of silicate ions, the content of Si ions in the N–A–S–H is notably increased (Si/Al=2.7 and Na/Al=1.5 ratio): The condensation degree increases and the mechanical strength increases too. Carbonate ions have however an opposite effect: The mechanical strength decreases due to a lesser reaction degree since the formation of sodium bicarbonate (trona and nahcolite) acidifies the system.

## Acknowledgements

Thanks to the Spanish Directorate General of Scientific Research for funding the project COO-1999-AX-038 and to the Regional Government of Madrid for awarding a post-doctoral grant associated with this research. And finally thanks to J.L. García and A. Gil for their co-operation in the mechanical tests.



## References

- [1] V.D. Glukhovskiy, G.S. Rostovskaja, G.V. Rumyna, High strength slag-alkaline cements, 7th Int. Cong. on the Chemistry of Cement, Paris, vol. 3, 1980, pp. 164–168.
- [2] P.V. Krivenko, Alkali cements, First International Conference of Alkaline Cements and Concretes, Ukraine, Kiev, 1994, pp. 12–129.
- [3] R.I.A. Malek, D.M. Roy, Structure and properties of alkaline activated cementitious materials, 97th annual meeting of the American Ceramic Society, Cincinnati, OH, 1995.
- [4] A. Palomo, M.W. Grutzeck, M.T. Blanco, Alkali activated fly ashes: a cement for the future, *Cem. Concr. Res.* 29 (8) (1999) 323–3329.
- [5] J.G.S. Van Jaarsveld, J.S.J. Van Deventer, Effect of the alkali metal activator on the properties of fly ash-based geopolymers, *Ind. Eng. Chem. Res.* 38 (10) (1999) 3932–3941.
- [6] F.F.V. Barbosa, J.D.K. MacKenzie, C. Thaumaturgo, Synthesis and characterisation of materials based on inorganic polymers of alumina and silica: sodium polysialate polymers, *Int. J. Inorg. Mater.* 2 (2000) 309–317.
- [7] Zhaohui Xie, X. Yunping, Hardening mechanisms of an alkaline-activated class F fly ash, *Cem. Concr. Res.* 31 (2001) 1245–1249.
- [8] A. Fernández-Jiménez, A. Palomo, Alkali-activated fly ashes: properties and characteristics, 11th International Congress on the Chemistry of Cement Durban, South Africa, 2003, pp. 1332–1340.
- [9] F. Puertas, A. Fernández-Jiménez, Mineralogical and microstructural characterisation of alkali-activated fly ash/slag pastes, *Cem. Concr. Comp.* (25) (2003) 287–292.
- [10] W.K.W. Lee, J.S.J. Van Deventer, Structural reorganization of class F fly ash in alkaline silicate solutions, *Colloids Surf., A Physicochem. Eng. Asp.* 211 (2002) 49–66.
- [11] A. Fernández-Jiménez, A. Palomo, Activation of Fly Ashes: A General View Eighth CANMET/ACI International Conference on Fly Ash, Silica Fume, Slag and Natural Pozzolans in Concrete, Las Vegas, U.S.A., SP-221-20, ISBN: 0-87031-146-8, (2004), pp. 351–365.
- [12] A. Fernández-Jiménez, A. Palomo, Characterisation of fly ashes. Potential reactivity as alkaline cements, *Fuel* 82 (2003) 2259–2265.
- [13] A. Palomo, S. Alonso, A. Fernández-Jiménez, I. Sobrados, J. Sanz, Alkaline activation of fly ashes. A  $^{29}\text{Si}$  NMR study of the reaction products, *J. Am. Ceram. Soc.* 87 (6) (2004) 1141–1145.
- [14] F. Mondragón, F. Rincón, L. Sierra, J. Escobar, J. Ramírez, J. Fernández, New perspectives for coal ash utilization: synthesis of zeolitic materials, *Fuel* 69 (1990) 263–266.
- [15] J.L. LaRosa, S. Kwan, M.W. Grutzeck, Zeolite formation in class F fly ash blended cement pastes, *J. Am. Ceram. Soc.* 75 (nº 6) (1992) 1574–1580.
- [16] N. Murayama, H. Yamamoto, J. Shibata, Mechanism of zeolite synthesis from coal fly ash by alkali hydrothermal reaction, *Int. J. Miner. Process.* 64 (2002) 1–17.
- [17] X. Querol, N. Moreno, J.C. Umaña, A. Alastuey, E. Hernández, A. López-Soler, F. Plana, Synthesis of zeolites from coal fly ash: on overview, *Int. J. Coal Geol.* (50) (2002) 413–423.
- [18] A. Palomo, A. Fernández-Jiménez, M. Criado, Geopolymers: same basic chemistry, different microstructures, *Mater. Constr.* 54 (2004) 77–91.
- [19] G. Steenbruggen, G.G. Hollman, The synthesis of zeolites from fly ash and the properties of the zeolite products, *J. Geochem. Explor.* 62 (1998) 305–309.
- [20] A. Fernández-Jiménez, A. Palomo, “Alkali activated fly ashes. Structural studies through Mid-Infrared Spectroscopy” *Microporous and Mesoporous Mat.* (in press, 2005).
- [21] W. Mozgawa, M. Sitarz, M. Rokita, Spectroscopic studies of different aluminosilicate structures, *J. Mol. Struct.* 511–512 (1999) 251–257.
- [22] A. Palomo, A. Fernández-Jiménez, Microstructural development of alkali-activated fly ash cement. A descriptive model, *Cem. Conc. and Research* (in press, 2005).
- [23] R. Kumar, A. Bhaumik, R. Kaur, S. Ganapathy, Promoter-induced enhancement of the crystallization rate of zeolites and related molecular sieves, *Nature* 381 (1996) 298–300.
- [24] Bhaumik, S.G. Hegde, R. Kumar, *Catal. Lett.* 35 (1995) 327–334.